RESEARCH ARTICLE
SOLID EARTH: SEISMOLOGY

Earth and Planetary Physics
8: 609–620, 2024
doi: 10.26464/epp2024039

Implementing and evaluating an automatic centroid moment tensor procedure for the Indonesia region and surrounding areas

Madlazim[1*], Muhammad Nurul Fahmi[1], Dyah Permata Sari[2], Ella Meilianda[3], and Sorja Koesuma[4]

[1]Physics Department, Faculty of Mathematics and Natural Sciences, Universitas Negeri Surabaya, Surabaya 60231, Indonesia;

[2]Science Education Study Program, Faculty of Mathematics and Natural Sciences, Universitas Negeri Surabaya 60231, Surabaya, Indonesia;

[3]Disaster Science Department, Faculty of Mathematics and Natural Sciences, Universitas Syiah Kuala, Aceh 23126, Indonesia;

[4]Physics Department, Faculty of Mathematics and Natural Sciences, Universitas Sebelas Maret, Solo 57126, Indonesia

Key Points:

- We applied an automatic, real-time centroid moment tensor (CMT) determination software program with local and regional data for Indonesia and the surrounding areas.
- The CMT solution in this study was compared with the Global CMT solution by using Kagan angles, with an average result of approximately 11.2°.
- Automatic and real-time CMT determination procedures were successfully implemented in Indonesia and the surrounding areas.

Citation: Madlazim, Fahmi, M. N., Sari, D. P., Meilianda, E., and Koesuma, S. (2024). Implementing and evaluating an automatic centroid moment tensor procedure for the Indonesia region and surrounding areas. *Earth Planet. Phys.*, *8*(4), 609–620. http://doi.org/10.26464/epp2024039

Abstract: The purpose of this research was to suggest an applicable procedure for computing the centroid moment tensor (CMT) automatically and in real time from earthquakes that occur in Indonesia and the surrounding areas. Gisola software was used to estimate the CMT solution by selecting the velocity model that best suited the local and regional geological conditions in Indonesia and the surrounding areas. The data used in this study were earthquakes with magnitudes of 5.4 to 8.0. High-quality, real-time broadband seismographic data were provided by the International Federation of Digital Seismograph Networks Web Services (FDSNWS) and the European Integrated Data Archive (EIDA) Federation in Indonesia and the surrounding areas. Furthermore, the inversion process and filter adjustment were carried out on the seismographic data to obtain good CMT solutions. The CMT solutions from Gisola provided good-quality solutions, in which all earthquake data had A-level quality (high quality, with good variant reduction). The Gisola CMT solution was justified with the Global CMT (GCMT) solution by using the Kagan angle value, with an average of approximately 11.2°. This result suggested that the CMT solution generated from Gisola was trustworthy and reliable. The Gisola CMT solution was typically available within approximately 15 minutes after an earthquake occurred. Once it met the quality requirement, it was automatically published on the internet. The catalog of local and regional earthquake records obtained through this technology holds great promise for improving the current understanding of regional seismic activity and ongoing tectonic processes. The accurate and real-time CMT solution generated by implementing the Gisola algorithm consisted of moment tensors and moment magnitudes, which provided invaluable insights into earthquakes occurring in Indonesia and the surrounding areas.

Keywords: centroid moment tensor; Gisola; International Federation of Digital Seismograph Networks Web Services (FDSNWS); real time; Indonesia

1. Introduction

Centroid moment tensors (CMTs) are computed automatically and in real time by using local or regional seismic wave data. Recently, earthquake monitoring agencies have promptly provided seismic waveform data directly and in real-time through broadband networks. Moreover, global earthquake data, such as those facilitated by the International Federation of Digital Seismograph Networks Web Services (FDSNWS), are made available by prominent entities, including the European Integrated Data Archive (EIDA) Federation (Strollo et al., 2021) and Japan's National Research Institute for Earth Sciences and Disaster Prevention, along with the Mediterranean Very Broadband Seismographic Network of the Istituto Nazionale di Geofisica e Vulcanologia, Italy.

Several software tools are presently used for moment tensor (MT) computations at regional distances, such as ISOLated Asperities (SIOLA) (Sokos and Zahradnik, 2008, 2013; Zahradník and Sokos, 2018) which was the first moment tensor inversion software widely used by seismologist, FMNEAR (Delouis, 2014), KInematic Waveform Inversion (KIWI; Cesca et al., 2010), and a program for

Correspondence to: Madlazim, madlazim@unesa.ac.id
Received 03 MAR 2024; Accepted 07 JUN 2024.
First Published online 03 JUL 2024.

moment tensor inversion of near-source seismograms developed by Yagi and Nishimura (2011), and ISOLated Asperities (ISOLA; Sokos and Zahradnik, 2008, 2013; Zahradník and Sokos, 2018). The automated inversion of the CMT was initially introduced in the European–Mediterranean region (Bernardi et al., 2004). The Incorporated Research Institutions for Seismology (IRIS) is the pioneer in establishing a robust, swift, and automated CMT computational framework. This innovation represents a critical service that earthquake- and tsunami-monitoring agencies should aim to provide. Accurate and prompt technology is being developed that will determine earthquake CMTs automatically and in real time for Indonesia and the surrounding areas. Inazu et al. (2016) developed a near-field tsunami forecast system based on near real-time seismic MT estimations in Indonesia, the Philippines, and Chile. However, these findings apply only to earthquakes with magnitudes of 7.5 to 8.6. Lauterjung and Letz (2017) founded an Indonesian Tsunami Early Warning System, but the system is prone to shortages, and it requires improvement because of errors (Madlazim and Prastowo, 2016). Triantafyllis et al. (2022) introduced the Gisola method, a high-performance computational tool for real-time CMT inversion. Yet despite its capabilities, Gisola has yet to be utilized for estimating CMT inversions of earthquakes in Indonesia and the surrounding areas in real time and automatically. Therefore, more effort and cautiousness are needed so that Gisola can be used to estimate the CMTs of earthquakes in Indonesia and the surrounding areas. We undertook the following efforts: (1) installing Gisola on a server (jokotingkir.ac.id) so that it could run in real time and automatically estimate CMTs for earthquakes; (2) setting the boundaries of a box-shaped region (GeoBox) to be limited to only the region of Indonesia and its surroundings, which are the subject of this research; (3) adjusting the velocity structure to be suitable for conditions in Indonesia and the surrounding areas; (4) adjusting the frequency band of earthquake waveforms according to the magnitude of the earthquake used for CMT inversion; and (5) identifying and processing three-component seismic waveforms from seismic stations for CMT inversions. Currently, Indonesia lacks the capacity for autonomous, real-time determination of earthquake CMTs, which results in substantial expenditures for this endeavor.

The availability of earthquake parameter information in a complete CMT, as our technology provides, is crucial for disaster mitigation. In addition, the earthquake CMT catalog generated by this technology is promising for improving the current understanding of regional seismicity and tectonics at the positions of ongoing earthquakes. Moment tensor solutions are readily available approximately 15 minutes after the earthquake parameters are available; they are then automatically published on the web. These CMT solutions are posted on the web once their quality is verified. With the technological innovations proposed in this research for automatic, real-time earthquake determination, Indonesia no longer needs to allocate considerable funds to pay foreign partners (other countries) for earthquake CMT data processing. The primary objective of this study is to suggest a tangible procedure capable of automatically identifying earthquake CMTs in real time for the purpose of mitigating earthquake disasters. This initiative marks an initial phase in establishing a tsunami warning system in Indonesia and the surrounding regions.

2. Literature Review

Several software programs have been developed for regional CMT inversion. One example is the TDMT_INV (Time Domain seismic Moment Tensor INVersion) software (Dreger, 2003) created by the Berkeley Seismology Laboratory at the University of California. This software has been adapted and enhanced to include additional features. Another tool, FMNEAR, has been integrated with the FDSNWS to enable automatic CMT determination (Triantafyllis and Evangelidis, 2019). ISOLA, which was initially designed for manual operation, has been extended to support automated functionality (Triantafyllis et al., 2013) and has been combined with the popular seismological suite SeisComP (Weber et al., 2007), resulting in a tool called Scisola (Triantafyllis et al., 2016). Recently, advances have been made in the development of fully automated tools for CMT inversion by utilizing a Bayesian framework (Vackář et al., 2017), as well as the development of new real-time algorithms (Jian PR et al., 2018) and efficient regional inversion routines based on SeisComP3 and the KIWI tool suite (Niksejel et al., 2021). Gisola, a high-performance computing application for real-time moment tensor inversion, has been successfully created (Triantafyllis et al., 2022). The findings presented by Triantafyllis et al. (2022) hold promise for advancing technology to automatically and promptly determine earthquake CMTs. These advances will have a substantial impact on earthquake and tsunami disaster mitigation efforts in Indonesia and the surrounding areas.

3. Materials and Methods

3.1 ADDIE Model

In this study, we utilized the ADDIE model (Aldoobie, 2015) to achieve our objectives. This model is composed of five stages: Analysis, Design, Development, Implementation, and Evaluation. Each stage of model development is described below:

(1) Analysis: This stage involved analyzing the need for technology development to determine earthquake CMTs automatically and in real time for disaster mitigation. The feasibility and quality requirements were also analyzed. Because the current system in Indonesia relies on foreign countries, achieving independence in disaster mitigation has yet to be realized.

(2) Design: The design stage focused on designing the technology for automatic, real-time earthquake CMT determination and served as the foundation for subsequent development processes. Figure 2 illustrates the design of the technology for automatic, real-time earthquake CMT determination.

(3) Development: Development within the ADDIE model entailed transforming the product design into a tangible realization. A conceptual framework was developed for applying automatic, real-time earthquake CMT determination technology in disaster mitigation, which resulted in a product ready for implementation:

(i) Installing Gisola on the jokotingkir.ac.id server so that it could run in real time and automatically estimate CMTs for earthquakes on a high-performance computer that had been provided.
(ii) Setting the GeoBox to include only the region of Indonesia and

the surrounding areas, which were the subject of this research.
(iii) Adjusting the velocity structure to be suitable for the conditions in Indonesia and its surroundings.
(iv) Adjusting the frequency band of the earthquake waveforms according to the magnitude of the earthquake used for CMT inversion.
(v) Identifying and installing three-component seismic stations to be used for earthquake CMT inversion.

(4) Implementation: At this stage, the automatic, real-time earthquake CMT determination technology was implemented in Indonesia and the surrounding areas. The initial evaluation was undertaken to gather feedback for future applications.

(5) Evaluation: Evaluation occurred throughout the process and at the end of each stage. Comprehensive evaluations were also conducted at the end of each of the four previous stages. Revisions were made to improve the application based on the evaluation results and unmet needs.

3.2 Moment Tensor Inversion

Earthquakes occur because of fault movements with specific characteristics, which can be identified based on the earthquake's MT. The MT describes the force direction causing the earthquake. At the Analysis stage of the ADDIE model, we formulated steps to determine solutions for the CMTs available in Indonesia and the surrounding areas. Our proposed technology resampled selected waveforms automatically and in real time, and it initiated calculations by adopting various parameters to ensure the quality of the CMT solutions. The variance reduction (VR) reflects the agreement between the observed and synthetic waveforms. Figure 1 depicts flowcharts of the automatic, real-time CMT determination process.

3.3 Calculation of Green's Functions

The calculation of Green's functions in this technology utilizes the Gisola software (Triantafyllis et al., 2022), an improved version of the Axitra utility, which supports multiprocessing on a CPU, resulting in faster computation times. Furthermore, this technology allows for the association of specific crustal models with geographic regions, known as GeoBox, as specified in the configuration. According to the initial event location, the technology selects the appropriate GeoBox and the corresponding crustal model. Additionally, this technology uses a three-dimensional (3D) spatial grid search method, wherein the number of trial source positions is determined around the initial hypocenter location. Unlike the GridMT method (Aki and Richards, 2002), which fixes the 3D grid of trial source positions to a specific geographic location, this approach provides greater flexibility in determining the distribution of trial source positions based on the user configuration. Multiple crustal models can be connected to multiple 3D grids and triggered simultaneously.

In such cases, the best MT solution, which achieves the highest VR, is selected. The 3D grid is defined based on the range and granularity of the epicentral distance and depth search, triggered by defined rules associated with the initial magnitude estimation. Operators have the ability to customize the range and density of the epicentral and depth dimensions of the grid, adapting it to the requirements of different applications, such as the minimum search criteria for moment magnitude (M_w) estimation, intermediate grids for real-time applications, or highly dense grids commonly used for research purposes. One of the processes followed in the Development stage of the ADDIE model is the selection of a velocity model suitable for the tectonic setting in Indonesia (see Table 1) as input for the Green's function calculations.

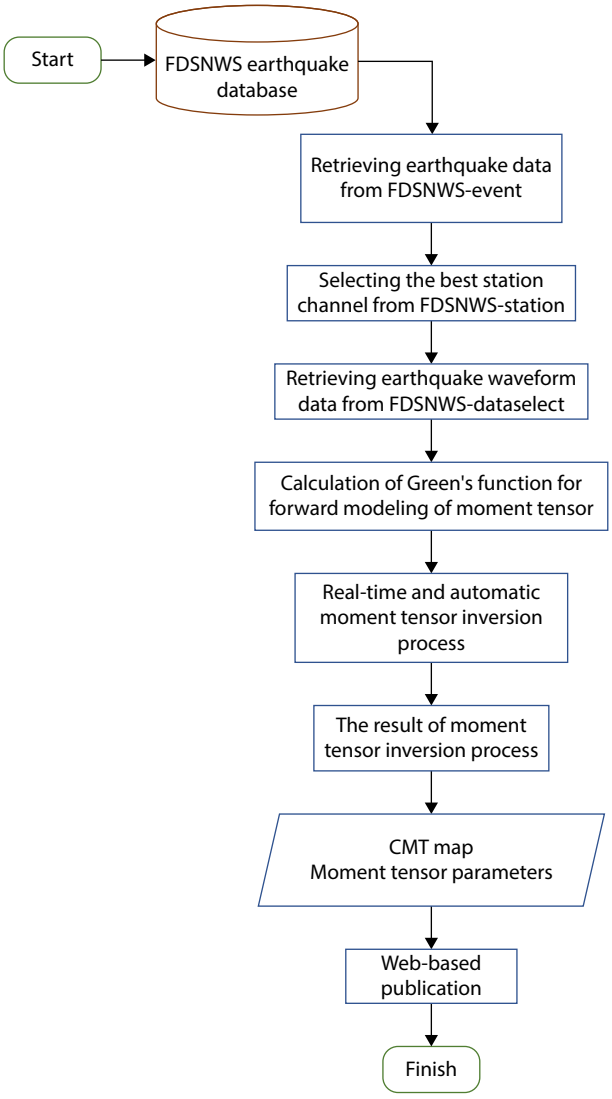

Figure 1. Flowchart of this technology. Determination of the CMT begins with the earthquake event, which is accessed from the FDSNWS real-time earthquake database. Next, local and regional station channels are selected, the three-component waveform is searched, and the Green's function is calculated to model the MT. Next, waveform inversion is performed and the quality of the inversion results is determined. The last step is to plot the output of the inversion results.

3.4 Inversion Computation

At the Development stage of the ADDIE model, one of the processes undertaken is inversion of an earthquake waveform. The initial steps involve the technology automatically sampling the selected waveforms and initiating computational calculations to obtain the CMT solutions. In addition to the customizable 3D

Table 1. One-dimensional velocity structure used to calculate the Green's functions.

Thickness (km)	V_P (km/s)	V_S (km/s)	ρ (g/cm^3)	Q_P	Q_S
2.0	3.50	2.00	2.00	500	300
6.0	4.30	2.43	2.37	500	300
14.0	6.05	3.41	2.70	500	300
17.5	6.88	3.94	2.95	500	300
63.5	8.00	4.50	3.31	500	300
150.0	8.15	4.66	3.32	500	300
100.0	8.30	4.80	3.35	500	300
100.0	9.00	5.14	3.65	500	300
100.0	9.60	5.49	3.84	500	300
100.0	10.30	5.89	4.07	500	300

Notes: V_P, P-wave velocity; V_S, S-wave velocity; ρ, density; Q_p, P-wave intrinsic attenuation, Q_s, S-wave intrinsic attenuation.

point source grid search, the operator can specify multiple customizable search ranges for center-of-mass time and multiple inversion frequency bands. In the case of multiple choices, the program will automatically select the MT solution with the highest VR. Finally, the user can revise the inversion procedure manually by changing the station selection and inversion frequency band without conducting the entire calculation from scratch. It should be noted that Gisola adopts various parameters by considering the quality of the MT solution. The VR reflects the match between observed and synthetic waveforms. The stability of the inversion is checked by using the condition number (CN) resulting from the ratio of the largest and smallest singular values (CN < 3–5, good inversion; CN > 10, unbalanced inversion; Křížová et al., 2013). In addition, the Focal Mechanism Variance Index reports the variability of the focal mechanism in the high correlation zone. In contrast, the Source Time Variance reports the stability of the solution in the spatiotemporal search (Zahradník and Sokos, 2018). In addition, an overall quality factor with an alphabetical part (A–D) based on the VR and the number of associated stations and a numerical part (1–4) based on the percentage share of compensated linear vector dipoles (Křížová et al., 2013) is reported. This analysis showed that solutions with A1 were the best, whereas those with D4 indicated unreliable solutions (Triantafyllis et al., 2022).

3.5 Automatic MT Computation Method

In this section, we describe the integration of the Development and Implementation stages of the ADDIE model. Here, we outline the main phases of the real-time and automatic waveform inversion procedure using Gisola software (Triantafyllis et al., 2022). The seven phases of automatic CMT computation are (1) CMT calculation triggering, (2) station metadata retrieval, (3) seismic waveform preprocessing, (4) station selection, based on azimuthal coverage and various quality metrics, (5) Green's function calculation, (6) inversion calculation, and (7) plotting and dissemination of the results. All these stages are summarized in Figure 2.

3.6 Data

The final stage of the ADDIE model is the Evaluation stage, during which we tested and evaluated 31 earthquake events in Indonesia by using data from our technology database, called Jokotingkir. The earthquake data were sourced from https://jokotingkir.unesa.ac.id/ and covered the period from July 2018 to July 2023. This time frame was selected based on the observed technological

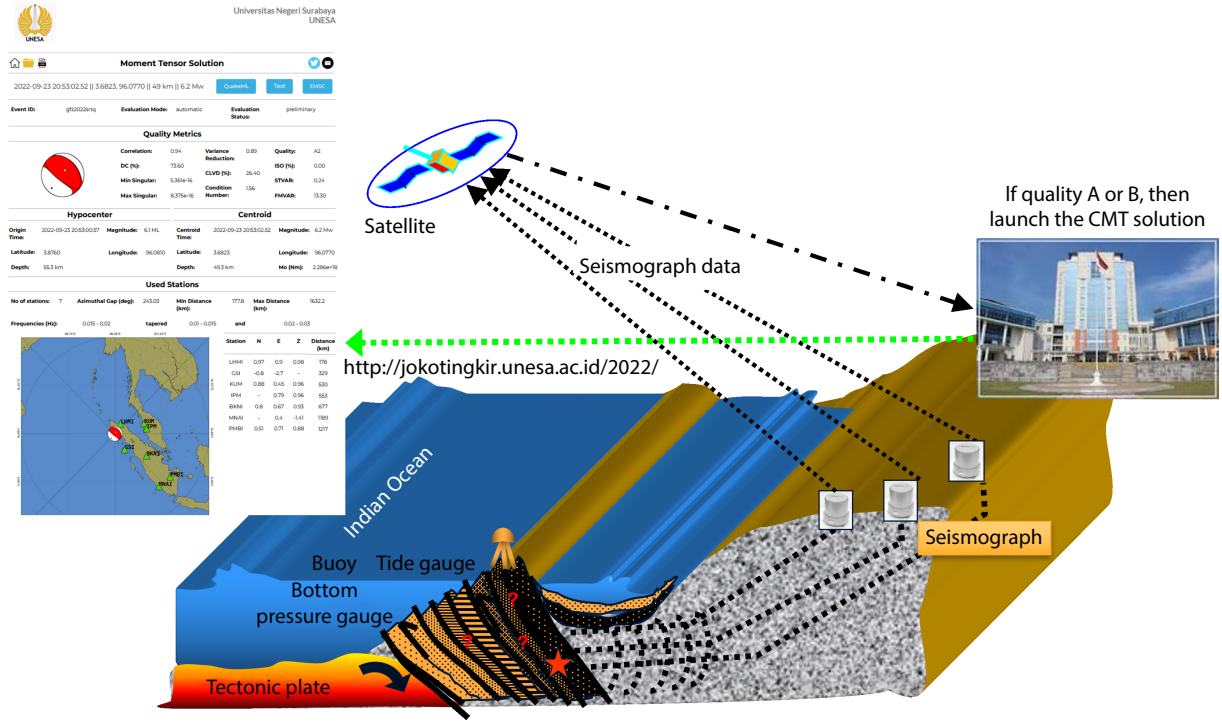

Figure 2. Technology design for automatic, real-time determination of earthquake CMT.

advances, transitioning from offline capabilities in 2018 to online and real-time capabilities being achieved by 2022 and continuing to the present. The dataset was constrained to earthquakes recorded by a minimum of four three-component seismic stations located within approximately 200 km of the epicenter. Thirty-one earthquake events in Indonesia and the surrounding regions were analyzed, with magnitudes ranging from M_w5.0 to 8.0. This magnitude range was chosen because CMT data processing from Gisola yielded more accurate solutions for earthquakes greater than M_w5.0. Seismic waveforms from earthquakes of this magnitude exhibited regional characteristics suitable for inversion. Additionally, the Gisola method implemented in Jokotingkir was used to compute the focal depth (H), fault parameters (strike, dip, and rake), and moment magnitude (M_w), as detailed in Table 2.

The earthquake seismographic recordings used for the inversion were provided by the existing FDSNWS seismic network in Indonesia, VG, the seismic network managed by the Indonesian Center for Volcanology and Geological Hazard Mitigation (see Figure 3; Pusat Vulkanologi dan Mitigasi Bencana Geologi, 2010). Currently, the VG network consists of more than 130 three-component, broadband, high-dynamic-range stations, all equipped with 40-second Trillium sensors and Trident digitizers, and with 29 stations consisting of high-broadband STS1 and STS2 sensors and 24-bit Quanterra data loggers.

The recorded waveforms were sampled at a rate of 100 samples

Table 2. Earthquake data utilized in this study, sourced from the Jokotingkir catalog.[a]

Event ID	Date	O.T. (hh: mm)	Lat (°)	Lon (°)	H (km)	Strike (°)	Dip (°)	Rake (°)	M_w
20180728	7/28/2018	22:47	−8.31	116.51	15	80	17	80	6.6
20180819	8/19/2018	14:56	−8.4	116.75	20	265	64	80	7.0
20181129	11/29/2018	20:21	0.21	96.89	8	312	47	−116	5.7
20190106	1/6/2019	17:27	2.48	126.63	40	209	50	96	6.6
20190412	4/12/2019	11:40	−1.85	122.56	8	310	78	42	6.8
20190624	6/24/2019	2:53	−6.51	129.17	246	158	75	−169	7.3
20190707	7/7/2019	15:08	0.55	126.10	24	226	72	137	6.9
20192410	10/24/2019	13:38	1.13	124.24	255	61	86	115	5.6
20200506	5/6/2020	13:53	−6.82	129.88	127	93	56	34	6.9
20200604	6/4/2020	8:49	2.98	128.15	142	127	49	10	6.5
20200706	7/6/2020	22:54	−5.69	110.55	506	309	68	−90	6.5
20200818	8/18/2020	22:24	−4.56	100.99	19	123	57	85	6.5
20200821	8/21/2020	4:09	−6.64	123.52	602	248	58	−71	6.7
20200906	9/6/2020	0:21	1.97	126.43	46	44	20	83	5.9
20200908	9/8/2020	0:45	−4.77	129.80	176	88	15	12	6.1
20210121	1/21/2021	12:23	5.04	127.30	117	189	73	97	7.0
20210514	5/14/2021	6:33	0.09	96.62	4	291	54	−137	6.9
20210811	8/11/2021	17:46	6.09	127.00	53	179	54	71	7.1
20211229	12/29/2021	18:26	−7.69	127.56	168	82	54	57	7.4
20220114	1/14/2022	9:05	−7.1	105.21	14	103	74	78	6.6
20220527	5/27/2022	2:36	−8.35	127.11	32	19	21	−140	6.3
20220723	7/23/2022	7:35	−7.57	122.44	10	269	43	93	5.5
20220823	8/23/2022	14:31	−5.3	102.92	47	119	65	79	6.2
20220923	9/23/2022	20:53	3.7	95.89	49	131	65	85	6.2
20221121	11/21/2022	6:21	−6.84	107.08	12	347	88	174	5.5
20221208	12/8/2022	0:50	−7.03	107.06	109	210	36	133	5.8
20230109	1/9/2023	12:26	−9.14	111.21	54	90	54	85	5.4
20230118	1/18/2023	0:34	0.02	123.2	146	66	56	94	6.1
20230402	4/2/2023	8:40	−7.77	118.66	14	161	78	164	5.6
20230415	4/15/2023	15:07	−5.06	102.78	52	120	62	79	5.6
20230607	6/7/2023	17:04	−9.13	110.72	16	149	81	102	5.7

[a]O.T., origin time; Lat, latitude; Lon, longitude, H, focal depth.

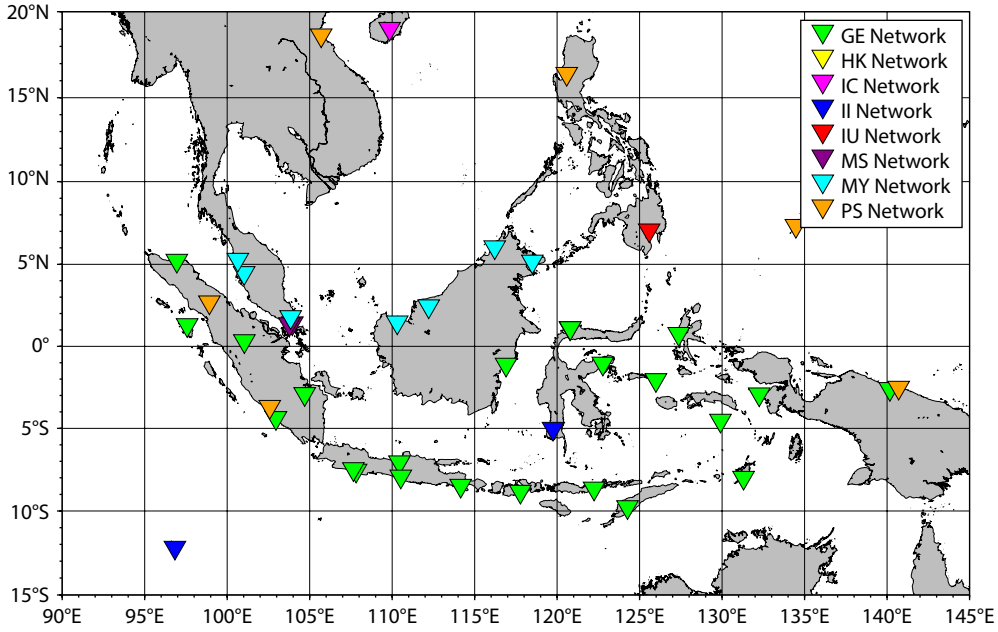

Figure 3. Station distribution map in this study.

per second and extracted within an 800-second window, commencing 3 minutes before the origin time of the event. Our aim in the selection of this window length was to minimize any potential artifacts resulting from the band-pass filtering applied to the signal toward the end of the window. It is important to note that despite the substantial window length, the automatic calculation remained efficient, as the triggering of the procedure guaranteed the availability of more than 10 minutes of data at all times.

4. Results and Discussion

This technology generated all CMT parameters, selected the best CMT solution based on the best VR, and distributed the solution (Figure 4).

In this final procedure, parallelized in the CPU domain, various plots were rendered for publication: (1) maps containing the contributing stations and the best focusing mechanism, (2) plots of displacement recordings, (3) plots with observed and synthetic waveforms, (4) extensive contour plots of the correlations at each spatiotemporal grid point, and (5) two vertical cross sections and one horizontal cross section of the 3D grid, for the best centroid time generated for each specific point (i.e., south to north, east to west) and map views. The CMT solutions were published in various

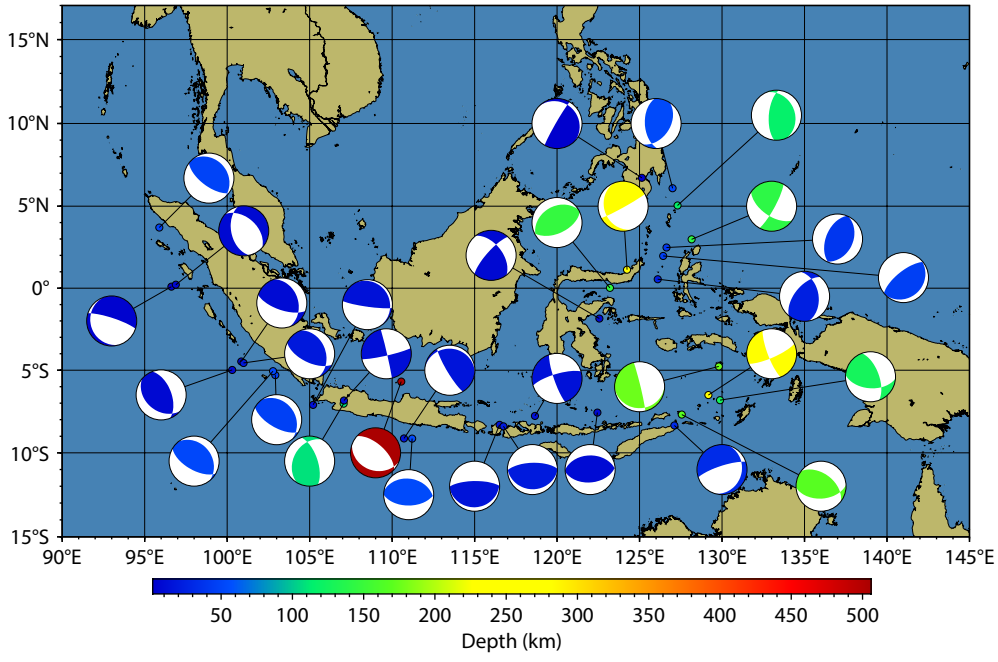

Figure 4. Distribution of earthquake data in Indonesia and the surrounding areas.

formats, such as QuakeML and SC3ML XML files, or ASCII text files, and all important information in the results was displayed on HTML web pages suitable for quick distribution and archiving, with automatically generated buttons for quick sharing via email or social media. In addition, registered recipients were automatically notified of the MT solution in their email accounts. Figure 5 shows the homepage with the software and displays real-time operations at Universitas Negeri Surabaya (UNESA). Optionally, the software could integrate the SeisComP FDSN Web Service to distribute MT solutions based on events from FDSNWS and archive them in the integrated SeisComP MySQL database (Triantafyllis et al., 2022).

4.1 Example of Automatic Moment Tensor Determination

To demonstrate the application of the procedure outlined earlier, we illustrate the Gisola CMT solution for two events (see Figure 6) with magnitudes of M_w 7.3 and 5.7, respectively. An earthquake with M_w 7.3 occurred on December 29, 2021, at 18:25:58.07 Coordinated Universal Time (UTC), with the latitude of the epicenter at −7.6290°, the longitude at 127.7111°, and the depth at 160.2 km in the Banda Sea, Indonesia. The active fault in the Banda Sea caused the earthquake, and the epicenter was located close to the Timor Leste Islands (Patria et al., 2021) , with M_w > 7.3. The second event with M_w 5.7 occurred on June 7, 2023, at 17:04:55.35 UTC, with the latitude of the epicenter at −8.9483°, the longitude at 110.5653°, and the depth at 16.0 km in the southern part of Java Island where there is a subduction zone.

The CMT solutions obtained from Jokotingkir for the first earthquake (M_w 7.3) and the second earthquake (M_w 5.7) revealed a reverse oblique fault type with dominance of the double-couple parameter exceeding 50%. This agreement aligns with the CMT solutions from the GCMT, as evidenced by the Kagan angle results for both earthquakes. The magnitude 7.3 earthquake exhibited a Kagan angle of 6.3°, whereas the M_w 5.7 earthquake had a Kagan angle of 7.5°. According to Pondrelli et al. (2006), if the Kagan angle values of two focal mechanisms are less than 60°, the results are considered similar. A reliable CMT solution, indicated by a high VR value, can be attributed to the azimuthal coverage of the recording stations. For the M_w 5.7 earthquake, the recording stations are predominantly located in the upper part (quadrants 1 and 2) of the earthquake because of the absence of recording stations in the southern part of the epicenter, which is in the ocean. However, despite this limitation, the agreement between the observed and calculated data from all the recording stations was quite satisfactory, resulting in a VR value of approximately 73%. As highlighted by Kumar et al. (2015), CMT solutions obtained from inversion when using a single station and the maximum azimuthal coverage of the stations can yield relatively similar results if agreement is high between the observed and calculated data. In contrast, the CMT solutions from Jokotingkir for both earthquakes were valid.

4.2 Evaluations

The visualization of the CMT solution from Gisola is represented by a blue beachball, in contrast to the red beachball representing the solution from the GCMT (refer to Table 3). The overall quality of the CMT solutions from all data, encompassing 31 earthquakes, exhibited an average quality value, falling within the range of A1 to A3, coupled with a VR value surpassing 60%. This correlation is associated with the appropriateness of the velocity model utilized

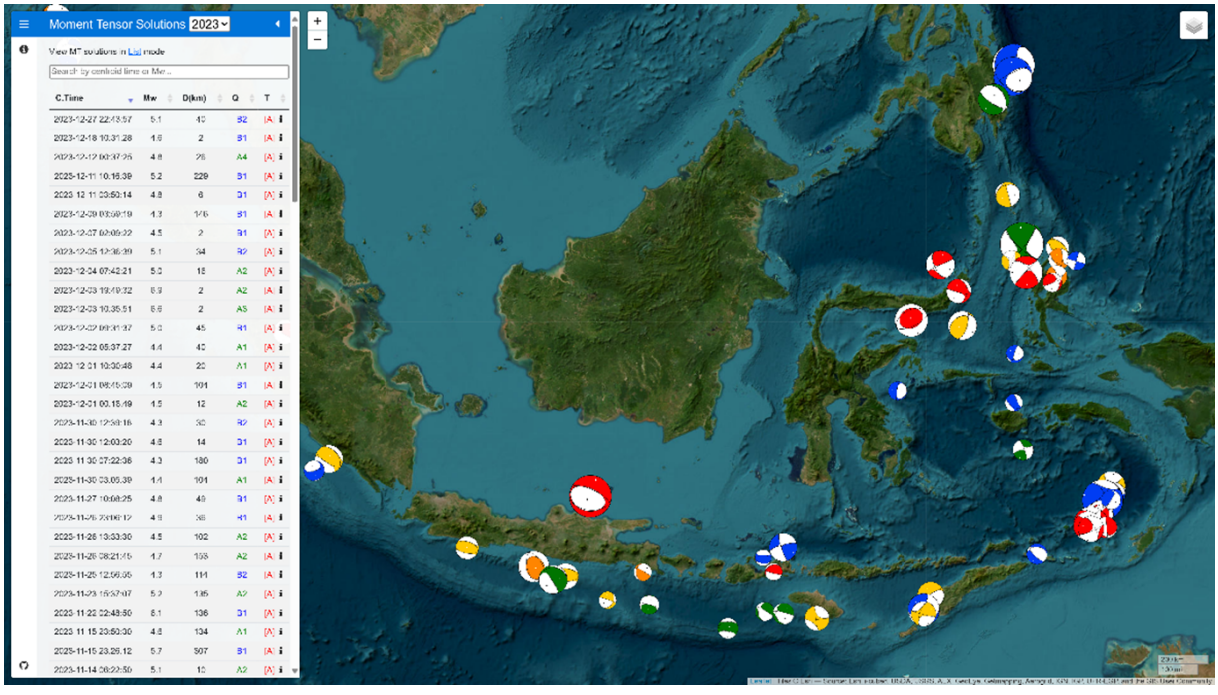

Figure 5. Screenshot of the homepage, which ships with this technology. Real-time operation at the Universitas Negeri Surabaya (UNESA) is shown. The CMT solutions are listed on the left and pinned on a map with a summary description. The user can search among solutions and be redirected to a detailed overview of each of them. The website accompanying this technology is freely accessible at http://jokotingkir.unesa.ac.id/.

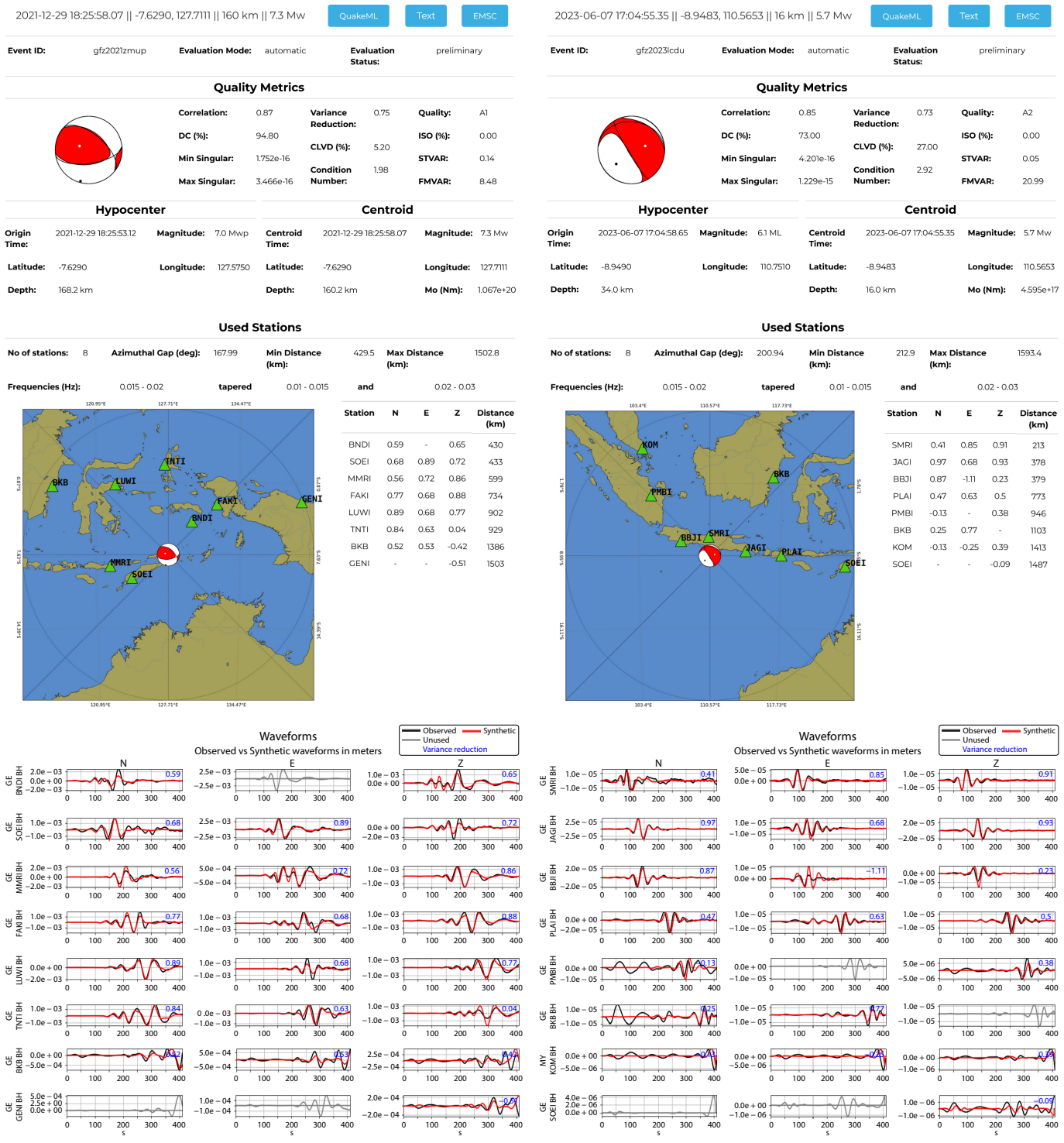

Figure 6. Example of the Gisola technology output. The left panel shows the CMT for the event on December 29, 2021 (UTC), with M_w of 7.3. The right panel shows the CMT for the event on June 7, 2023 (UTC), with M_w of 5.7.

as input in Gisola, which aligned with the characteristics of Indonesia and the surrounding areas. Additionally, each earthquake was recorded by a station with a favorable azimuthal alignment, as established by Dreger and Helmberger (1993) and D'Amico et al. (2010, 2011). However, it is essential to note that relying solely on these quality parameters cannot guarantee complete confidence in the MT solution. Consequently, the justification of the CMT solution from other pertinent sources is imperative to ensure the validity and accuracy of the results obtained.

One way of assessing the effectiveness of this technology is to compare the concordance of CMT source parameters between Gisola and the GCMT. The GCMT, a well-established platform, provides CMT solutions based on teleseismic data (Ekström et al., 2012). The CMT parameter results from Jokotingkir, including latitude, longitude, magnitude, centroid depth, origin time, strike,

Table 3. Results of the Kagan angle of earthquakes in Indonesia and the surrounding areas with a magnitude (M_w) > 5 recorded from July 2018 to July 2023.

Event ID	Location	GCMT	Gisola	Quality	Kagan angle (°)
20180819	SUMBAWA REGION			A1	5.6
20190106	MOLUCCA SEA			A2	6.1
20211229	BANDA SEA			A1	6.3
20220923	NORTHERN SUMATRA			A2	6.4
20200908	BANDA SEA			A1	6.5
20200604	HALMAHERA			A1	6.6
20221208	JAVA			A1	7.3
20200906	MOLUCCA SEA			A1	7.4
20230607	SOUTHERN JAVA			A2	7.5
20192410	SULAWESI			A1	7.8
20220823	SOUTHERN SUMATRA			A2	8.0
20180728	SUMBAWA REGION			A1	8.3
20200506	BANDA SEA			A1	8.6
20230402	FLORES SEA			A1	8.8
20230109	JAVA			A3	9.2
20230118	SULAWESI			A3	9.3
20230415	SOUTHERN SUMATRA			A2	10.0
20210811	MINDANAO			A2	10.9
20220114	SUNDA STRAIT			A2	11.1
20221121	JAVA			A2	11.1
20210121	TALAUD ISLANDS			A2	11.4
20210514	NORTHERN SUMATRA			A2	13.5
20220723	FLORES SEA			A1	14.2
20200818	SOUTHERN SUMATRA			A2	17.2
20181129	NORTHERN SUMATRA			A1	17.5
20220527	TIMOR REGION			A2	19.9
20200706	JAVA SEA			A1	23.0
20200821	BANDA SEA			A2	33.5
20190412	SULAWESI INDONESIA			A3	—
20190624	BANDA SEA			A3	—
20190707	MOLUCCA SEA			A3	—

dip, and rake, were compared with parameters from the GCMT. Furthermore, the Kagan angle (Kagan, 1991) was used to quantitatively assess the agreement between the Jokotingkir CMT solutions (only double-couple earthquakes) and the GCMT. The Kagan angle indicates the amount of rotation needed to align one double-couple earthquake source with another, and it can range from 0° (indicating absolute agreement) to 120° (denoting complete disagreement). Consequently, a value less than 60° suggests acceptable correspondence, whereas a value greater than 60° implies a mismatch (Pondrelli et al., 2006).

Furthermore, Figure 7 depicts a comparison of earthquake source parameters obtained from Jokotingkir and the GCMT for 31 earthquakes. The match of strike, dip, rake, and M_w parameter data between Jokotingkir and the GCMT yielded root mean square error (RMSE) values of 5.3, 7.0, 13.8, and 0.09, respectively. In addition, the R^2 values for the three parameters were 0.996, 0.876, 0.977, and 0.975. It is noteworthy that the dip angle parameter exhibited the largest RMSE value. This peculiarity can be attributed to the application of different methods in the parameter calculation process, with Gisola relying on regional data and the GCMT utilizing teleseismic data.

According to the results of the Kagan angle analysis for all earthquakes with double-couple components (28 earthquakes), the angles ranged from 5.6 to 33.5 (see Table 3). The histogram of the Kagan angles shows that the dominant values lie in the range of 5° to 10° (see Figure 8). This indicates a good result for the CMT solution comparison between Jokotingkir and the GCMT. Three earthquakes are not included in the Kagan angle analysis, specifically those listed in Table 3, three from the last. This exclusion arises from the dominant compensated linear vector dipole component in these earthquakes. Nevertheless, these three earthquakes possessed A3 quality, indicating good results, and the evaluation of other parameters for these earthquakes was conducted. In addition, in terms of fault type, the non-double-couple solution generated from this study had fairly good agreement with the GCMT solution, which was characterized by almost the same beachball. This exclusion was necessary because the Kagan angle is specifically suitable for comparing full MT solutions with double-couple components (Kagan, 1991; Lee SJ et al., 2014). The evaluation based on the Kagan angle yielded an average value of 11.2° for the 29 earthquakes, with a total similarity level of 90.1%. However, two CMT solutions exhibited significant deviations in Kagan angle values compared with others. Specifically, event ID 20200706 showed an angle of 23.0°, and event ID 20200821 had a value of 33.5°. The reason for these differences is that both earthquakes occurred at a very deep depth (>500 km), resulting in a suboptimal performance grid-search process of the real-time CMT processing method.

We also compared the source parameters based on the location of the earthquakes. Figure 9 illustrates the overall difference between the Jokotingkir CMT and the GCMT. In terms of the horizontal position of the earthquake (see Figures 9a and 9b), which included the parameters of latitude and longitude, the difference

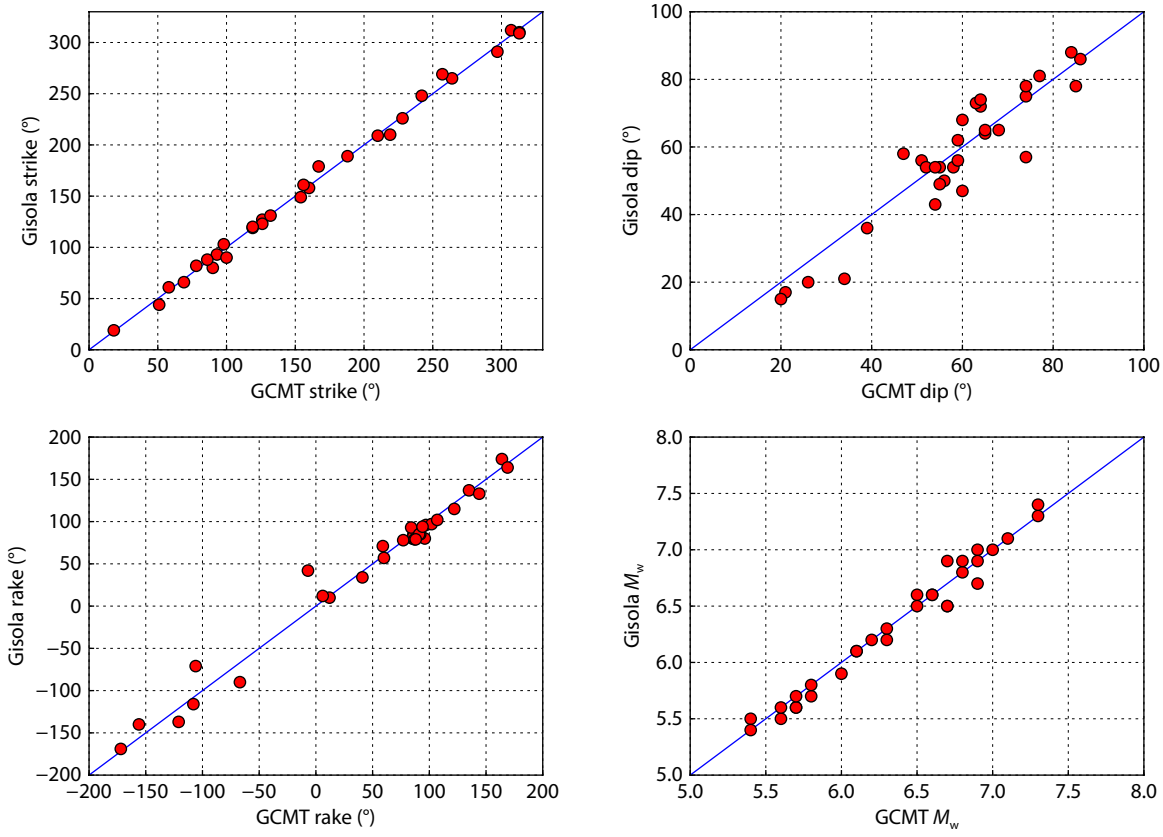

Figure 7. Scatter plot of CMT parameters between Gisola and the GCMT. The top left panel represents the strike angle, the top right panel is the dip angle, the bottom left panel denotes the rake angle, and the bottom right panel is M_w.

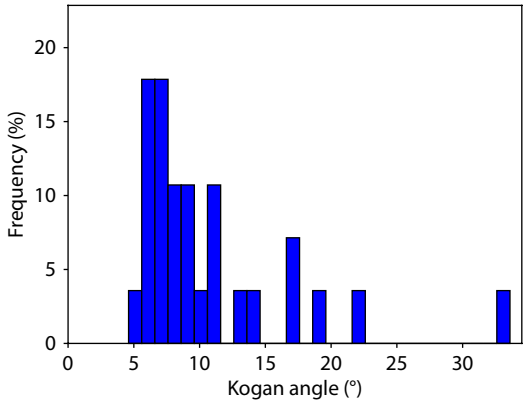

Figure 8. Histogram of the Kagan angle comparison between the Jokotingkir CMT and the GCMT.

was minimal, typically approximately ±0.1°, with an average value close to 0.0° for both latitude and longitude. Specifically, the mean value for latitude was 0.03, whereas for longitude, it was 0.07. A significant disparity was observed in the vertical component, where the difference ranged from ±30°, with an average value of −3.37° (see Figure 9c). Again, this substantial difference in the centroid depth parameter was primarily attributable to the suboptimal grid-search process, particularly for deep earthquakes, within the framework of a real-time monitoring system. Furthermore, Figure 9d elucidates the disparity in origin time between the Jokotingkir and GCMT earthquake events. Notably, there was no significant difference in this parameter, with an average value of approximately −3.9 seconds. This relatively small time difference can be attributed to the temporal resolution of the Jokotingkir real-time system, which is consistently updated with monitoring intervals of approximately 4 to 5 seconds.

In general, the differences in all source parameters between Jokotingkir and the GCMT demonstrated good agreement. Focal mechanism parameters, such as strike, dip, and rake, yielded satisfactory results, with an average root mean square error (RMSE) value of approximately 8.9. Similarly, the comparison of magnitude (M_w) between Jokotingkir and the GCMT indicated a high level of agreement. Moreover, other source parameters, including the latitude, longitude, centroid depth, and origin time, exhibited good agreement without significant bias.

Future improvements will include prioritizing enhancement of the grid-search process, especially for deep earthquakes, and refining the computational algorithms to achieve faster and more accurate CMT solutions. Nevertheless, the findings of this study lay a solid foundation for the development of a computational system ready to determine CMT solutions quickly and accurately in Indonesia and the surroundings areas.

5. Conclusions

The implementation of the Gisola algorithm is an automated and real-time solution for determining CMTs of earthquakes in the region of Indonesia and the surrounding areas. We aimed to facili-

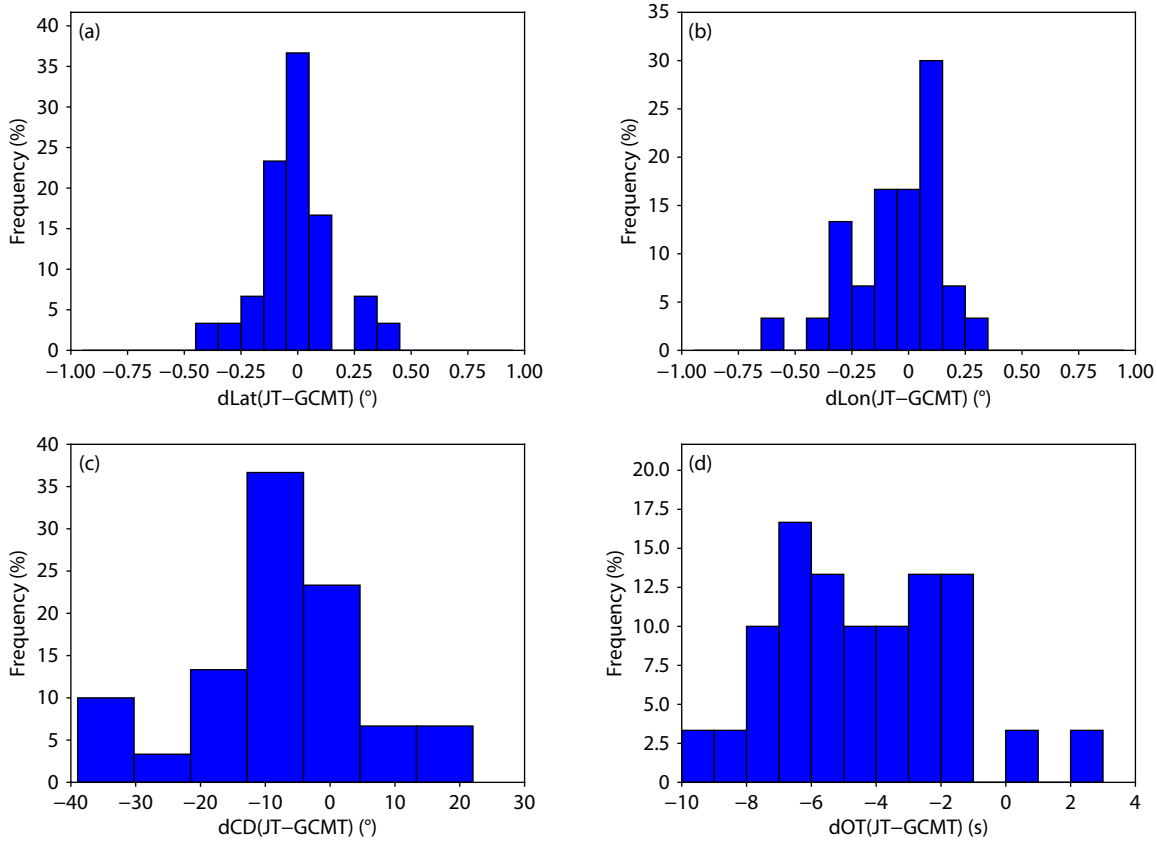

Figure 9. Comparison of source parameters for the location and origin time of the earthquakes. Histogram of (a) the difference in latitude, (b) the difference in longitude, (c) the difference in centroid depth, and (d) the difference in the earthquake origin time.

tate the timely and automatic determination of CMT parameters for regional seismic events. The CMT computational methodology leverages the foundational principles of the Gisola software, coupled with the real-time event notification system offered by the FDSNWS. According to the results of the Kagan angle analysis, the average Kagan angle value was 11.2°, and the results of the CMT source parameter comparison between Jokotingkir and the GCMT were found to be in good agreement.

Acknowledgments

The authors sincerely thank N. Triantafyllis for providing the Gisola software and guiding us in its use. The authors also extend their thanks to the FDSNWS and the EIDA Federation for providing the seismic stations in Indonesia. Additionally, appreciation is extended to Universitas Negeri Surabaya, Universitas Sebelas Maret, and Universitas Syiah Kuala for providing research grants for the Indonesian Collaborative Research (RKI) scheme.

References

Aki, K., and Richards, P. G. (2002). *Quantitative Seismology* (2nd ed). Sausalito, California: University Science Books.

Aldoobie, N. (2015). ADDIE model. *Am. Int. J. Contemp. Res.*, *5*(6), 68–72.

Bernardi, F., Braunmiller, J., Kradolfer, U., and Giardini, D. (2004). Automatic regional moment tensor inversion in the European–Mediterranean region. *Geophys. J. Int.*, *157*(2), 703–716. https://doi.org/10.1111/j.1365-246X.2004.02215.x

Cesca, S., Heimann, S., Stammler, K., and Dahm, T. (2010). Automated procedure for point and kinematic source inversion at regional distances. *J. Geophys. Res.: Solid Earth*, *115*(B6), B065304. https://doi.org/10.1029/2009JB006450

D'Amico, S., Orecchio, B., Presti, D., Gervasi, A., Zhu, L., Guerra, I., Neri, G., and Herrmann, R. (2011). Testing the stability of moment tensor solutions for small earthquakes in the Calabro-Peloritan Arc region (southern Italy). *Boll. Geofis. Teor. Appl.*, *52*(2), 1–16. https://doi.org/10.4430/bgta0009

D'Amico, S., Orecchio, B., Presti, D., Zhu, L. P., Herrmann, R. B., and Neri, G. (2010). Broadband waveform inversion of moderate earthquakes in the Messina Straits, southern Italy. *Phys. Earth Planet. Int.*, *179*(3-4), 97–106. https://doi.org/10.1016/j.pepi.2010.01.012

Delouis, B. (2014). FMNEAR: Determination of focal mechanism and first estimate of rupture directivity using near-source records and a linear distribution of point sources. *Bull. Seismol. Soc. Am.*, *104*(3), 1479–1500. https://doi.org/10.1785/0120130151

Dreger, D. S., and Helmberger, D. V. (1993). Determination of source parameters at regional distances with three-component sparse network data. *J. Geophys. Res.: Solid Earth*, *98*(B5), 8107–8125. https://doi.org/10.1029/93JB00023

Dreger, D. S. (2003). 85.11-TDMT_INV: Time Domain seismic Moment Tensor INVersion. *Int. Geophys.*, *81*, 1627. https://doi.org/10.1016/S0074-6142(03)80290-5

Ekström, G., Nettles, M., and Dziewoński, A. M. (2012). The global CMT project 2004–2010: Centroid-moment tensors for 13,017 earthquakes. *Phys. Earth Planet. In.*, *200–201*, 1–9. https://doi.org/10.1016/j.pepi.2012.04.002

Inazu, D., Pulido, N., Fukuyama, E., Saito, T., Senda, J., and Kumagai, H. (2016). Near-field tsunami forecast system based on near real-time seismic moment tensor estimation in the regions of Indonesia, the Philippines, and Chile. *Earth, Planets Space*, *68*(1), 73. https://doi.org/10.1186/s40623-016-0445-x

Jian, P. R., Tseng, T. L., Liang, W. T., and Huang, P. H. (2018). A new automatic full-waveform regional moment tensor inversion algorithm and its applications in the Taiwan area. *Bull. Seismol. Soc. Am.*, *108*(2), 573–587. https://doi.org/10.1785/0120170231

Kagan, Y. Y. (1991). 3-D rotation of double-couple earthquake sources. *Geophys. J. Int.*, *106*(3), 709–716. https://doi.org/10.1111/j.1365-246X.1991.tb06343.x

Křížová, D., Zahradník, J., and Kiratzi, A. (2013). Resolvability of isotropic component in regional seismic moment tensor inversion. *Bull. Seismol. Soc. Am.*, *103*(4), 2460–2473. https://doi.org/10.1785/0120120097

Kumar, R., Gupta, S. C., and Kumar, A. (2015). Effect of azimuthal coverage of an earthquake on moment tensor solutions estimated by waveform inversion. *Arab. J. Geosci.*, *8*(8), 5713–5726. https://doi.org/10.1007/s12517-014-1666-6

Lauterjung, J., and Letz, H. (2017). *10 Years Indonesian Tsunami Early Warning System: Experiences, Lessons Learned and Outlook*. Potsdam, Germany: GFZ German Research Centre for Geosciences.

Lee, S. J., Liang, W. T., Cheng, H. W., Tu, F. S., Ma, K. F., Tsuruoka, H., Kawakatsu, H., Huang, B. S., and Liu, C. C. (2014). Towards real-time regional earthquake simulation I: Real-time moment tensor monitoring (RMT) for regional events in Taiwan. *Geophys. J. Int.*, *196*(1), 432–446. https://doi.org/10.1093/gji/ggt371

Madlazim, and Prastowo, T. (2016). Evaluation of earthquake parameters used in the Indonesian Tsunami Early Warning System. *Earthq. Sci.*, *29*(1), 27–33. https://doi.org/10.1007/s11589-016-0143-6

Niksejel, A., Shomali, Z. H., Cesca, S., and Moradi, A. (2021). Towards a regional, automated full moment tensor inversion for medium to large magnitude events in the Iranian plateau. *J. Seismol.*, *25*(2), 653–669. https://doi.org/10.1007/s10950-020-09967-8

Patria, A., Tsutsumi, H., and Natawidjaja, D. H. (2021). Active fault mapping in the onshore northern Banda Arc, Indonesia: Implications for active tectonics and seismic potential. *J. Asian Earth Sci.*, *218*, 104881. https://doi.org/10.1016/j.jseaes.2021.104881

Pondrelli, S., Salimbeni, S., Ekström, G., Morelli, A., Gasperini, P., and Vannucci, G. (2006). The Italian CMT dataset from 1977 to the present. *Phys. Earth Planet. Int.*, *159*(3-4), 286–303. https://doi.org/10.1016/j.pepi.2006.07.008

Pusat Vulkanologi dan Mitigasi Bencana Geologi. (2010). *VG: Seismic Network of the Indonesian Center for Volcanology and Geological Hazard Mitigation* [Data set]. https://doi.org/10.7914/SN/VG

Sokos, E. N., and Zahradnik, J. (2008). ISOLA a Fortran code and a Matlab GUI to perform multiple-point source inversion of seismic data. *Comput. Geosci.*, *34*(8), 967–977. https://doi.org/10.1016/j.cageo.2007.07.005

Sokos, E., and Zahradnik, J. (2013). Evaluating centroid-moment-tensor uncertainty in the new version of ISOLA software. *Seismol. Res. Lett.*, *84*(4), 656–665. https://doi.org/10.1785/0220130002

Strollo, A., Cambaz, D., Clinton, J., Danecek, P., Evangelidis, C. P., Marmureanu, A., Ottemöller, L., Pedersen, H., Sleeman, R., … Triantafyllis, N. (2021). EIDA: The European Integrated Data Archive and service infrastructure within ORFEUS. *Seismol. Res. Lett.*, *92*(3), 1788–1795. https://doi.org/10.1785/0220200413

Triantafyllis, N., Sokos, E., and Ilias, A. (2013). Automatic moment tensor determination for the Hellenic Unified Seismic Network. *Bull. Geol. Soc. Greece*, *47*(3), 1308–1315. https://doi.org/10.12681/bgsg.10912

Triantafyllis, N., Sokos, E., Ilias, A., and Zahradník, J. (2016). Scisola: Automatic moment tensor solution for SeisComP3. *Seismol. Res. Lett.*, *87*(1), 157–163. https://doi.org/10.1785/0220150065

Triantafyllis, N., and Evangelidis, C. (2019). FDSN Web Services integrated with automatic moment tensor calculation. In *Proceedings of the EGU General Assembly 2019*. EGU. https://doi.org/10.13140/RG.2.2.20236.16006

Triantafyllis, N., Venetis, I. E., Fountoulakis, I., Pikoulis, E.V., Sokos, E., and Evangelidis, C. P. (2022). Gisola: A high-performance computing application for real-time moment tensor inversion. *Seismol. Res. Lett.*, *93*(2A), 957–966. https://doi.org/10.1785/0220210153

Vackář, J., Burjáanek, J., Gallovič, F., Zahradńik, J., and Clinton, J. (2017). Bayesian ISOLA: New tool for automated centroid moment tensor inversion. *Geophys. J. Int.*, *210*(2), 693–705. https://doi.org/10.1093/gji/ggx158

Weber, B., Becker, J., Hanka, W., Heinloo, A., Hoffmann, M., Kraft, T., Pahlke, D., Reinhardt, J., and Thoms, H. (2007). *SeisComP3—Automatic and Interactive Real Time Data Processing*. Vienna, Austria: General Assembly European Geosciences Union (EGU).

Yagi, Y., and Nishimura, N. (2011). Moment tensor inversion of near source seismograms. *Bull. Int. Inst. Seismol. Earthq. Eng.*, *45*, 133–138.

Zahradník, J., and Sokos, E. (2018). ISOLA code for multiple-point source modeling—Review. In S. D'Amico (Ed.), *Moment Tensor Solutions: A Useful Tool for Seismotectonics* (pp. 1–28). New York: Springer. https://doi.org/10.1007/978-3-319-77359-9_1